Journal of proteome research

Article

pubs.acs.org/jpr

Impact of the Pd_2Spermine Chelate on Osteosarcoma Metabolism: An NMR Metabolomics Study

Inês Lamego,[†,‡] M. Paula M. Marques,[‡,§] Iola F. Duarte,[†] Ana S. Martins,[†] Helena Oliveira,[∥] and Ana M. Gil*[,†]

[†]Department of Chemistry and CICECO-Aveiro Institute of Materials, (CICECO/UA), University of Aveiro, 3810 Aveiro, Portugal

[‡]R&D Unit "Molecular Physical-Chemistry", University of Coimbra, 3000-213 Coimbra, Portugal

[§]Department of Life Sciences, Faculty of Science and Technology, University of Coimbra, 3000-213 Coimbra, Portugal

[∥]Department of Biology & CESAM, University of Aveiro, 3810 Aveiro, Portugal

Supporting Information

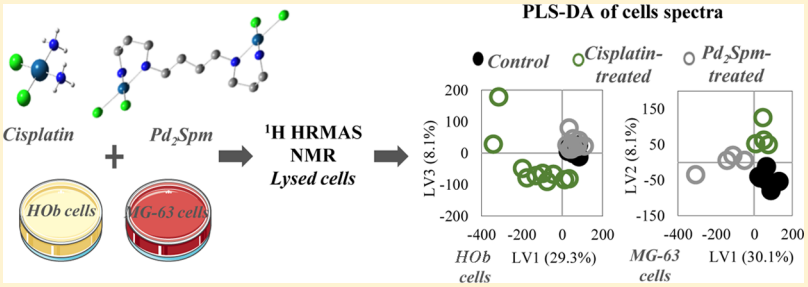

ABSTRACT: A metabolomics study of Pd_2Spermine(Spm) on osteosarcoma MG-63 and osteoblastic HOb cells is presented to assess the impact of the potential palladium drug on cell metabolism compared with cisplatin (cDDP). Despite its higher cytotoxicity, Pd_2Spm induced lower (and reversible) metabolic impact on MG-63 cells and the absence of apoptosis; conversely, it induced significant deviations in osteoblastic amino acid metabolism. However, when in combination with doxorubicin and methotrexate, Pd_2Spm induced strong metabolic deviations on lipids, choline compounds, amino acids, nucleotides, and compounds related to antioxidative mechanisms (e.g., glutathione, inositol, hypoxanthine), similarly to the cDDP cocktail. Synergetic effects included triggering of lipid biosynthesis by Pd_2Spm in the presence of doxorubicin (and reinforced by methotrexate) and changes in the glycosylation substrate uridine diphosphate acetylgalactosamine and methionine and serine metabolisms. This work provides promising results related to the impact of Pd_2Spm on osteosarcoma cellular metabolism, particularly in drug combination protocols. Lipid metabolism, glycosylation, and amino acid metabolisms emerge as relevant features for targeted studies to further understand a potential anticancer mechanism of combined Pd_2Spm.

KEYWORDS: *palladium anticancer drugs, osteosarcoma, osteoblasts, metabolomics, NMR*

INTRODUCTION

The serendipitous discovery of the antitumor activity of cisplatin (*cis*-diamminedichloroplatinum(II), *cis*-$Pt(NH_3)_2Cl_2$, cDDP) (Figure 1a, left),[1] a deoxyribonucleic acid (DNA)-targeting agent causing apoptotic cell death (through intra- and interstrand DNA cross-links), fostered its clinical introduction in 1978 as the first successful metal-based anticancer drug.[2] This triggered extensive interest in inorganic compounds as potential antineoplastic agents and platinum complexes (namely, cisplatin, carboplatin, and oxaliplatin) are among the most efficient chemotherapeutic agents in clinical use today. However, research still focuses on their cytotoxicity mechanisms to enhance antitumor capacity and reduce deleterious side effects, such as severe systemic toxicity and acquired resistance.[3] Therefore, many unconventional Pt(II) and Pt(IV) compounds have been tested,[4] mainly based on pre-established structure−activity relationships (SARs) as well as other metal complexes, for example, containing ruthenium (Ru(II) and Ru(III)),[5,6] titanium (Ti(IV)),[7] and gold (Au(I) and Au(III)).[8] Palladium (Pd) compounds have also drawn particular attention due to the similarity to Pt(II) (electronic structure and coordination chemistry),[9,10] and such agents have shown favorable cytotoxicity activity, despite their high lability (ca. 10^5 times higher than Pt(II) analogues).[11−13] The in vivo stability of Pd(II) antitumor agents relies on strongly coordinating ligands (e.g., dithiocarbamates, polydentate linear amines) and reasonably nonlabile leaving group(s).[14,15] In this context, cisplatin-like polynuclear Pd(II) chelates with linear amines have been shown to trigger increased DNA damage through nonconventional interactions (long-distance intra- and interstrand covalent and noncovalent cross-links) mainly with purines[16−18] while hindering effective DNA repair mechanisms and thus circumventing acquired drug resistance.[19] Polyamine

Received: January 18, 2017
Published: February 28, 2017

DOI: 10.1021/acs.jproteome.7b00035
J. Proteome Res. 2017, 16, 1773−1783

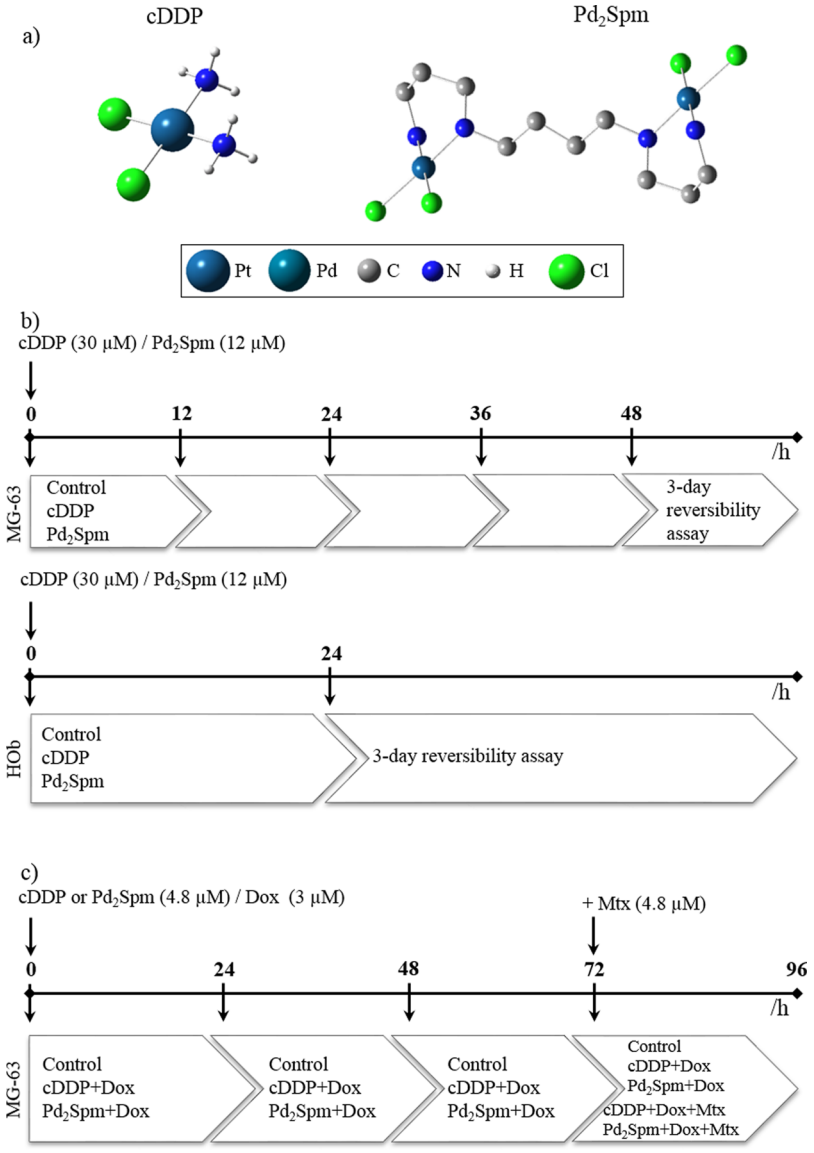

Figure 1. (a) Chemical structures of cDDP and Pd_2Spm. Schematic representations of the protocols followed for: (b) single administration of either Pd_2Spm (12 μM) and cDDP (30 μM) to MG-63 and HOb cells (two independent assays with duplicates) and (c) combined administration of cDDP (4.8 μM)/Dox (3 μM)/Mtx (4.8 μM) or Pd_2Spm (4.8 μM)/Dox (3 μM)/Mtx (4.8 μM) to MG-63 cells (three independent assays with duplicates). The vertical arrows indicate the time points at which viability was assessed.

ligands comprise biogenic amines (e.g., spermine, Spm, $H_2N(CH_2)_3NH(CH_2)_4NH(CH_2)_3NH_2$), which play a crucial role in cell growth and differentiation.[20] The Pd_2SpmCl_2 (or Pd_2Spm) complex (Figure 1a, right) has displayed promising antitumor properties[21] and, more recently, higher efficacy against human ovarian carcinoma (A2780 cells) than its Pt(II) counterpart (although still less efficient than cDDP), with both chelates displaying favorable cytotoxicity toward a cDDP-resistant cell line.[22] In addition, Pd_2Spm cytotoxicity in triple-negative human breast adenocarcinoma (MDA-MB-231 cell line) was higher than that of cDDP, the latter being, however, more effective in estrogen-responsive breast cancer (MCF-7 cells).[11] Substitution of Pt(II) by Pd(II) in the dinuclear Spm complex was seen to increase cytotoxicity toward a human oral squamous cell carcinoma (HSC-3),[23] and, similarly to cDDP, Pd_2Spm was shown to trigger histone H2A (H2AX variant) phosphorylation and act on the cytoskeleton, thus influencing cell morphology and division.[11] The formation of stable Pd_2Spm/DNA adducts has been demonstrated, prompting distinctive morphological changes in *ds*DNA.[24]

Building up on the above results and considering the modest success of the currently available treatment options for osteosarcoma (the most common primary bone tumor in children and adolescents), evaluation of Pd_2Spm on this high-incidence cancer is of undisputable relevance. The evaluation of the detailed metabolic impact of the agent on the target cells through metabolomics is a powerful strategy to obtain information on drug mechanisms and triggered cellular adaptations, thus potentially providing information on cellular resistance or positive response. The increasing number of metabolomic studies of anticancer agents (particularly metal complexes) has focused mainly on cell extracts but also exploited the use of high-resolution magic-angle spinning (HRMAS) nuclear magnetic resonance (NMR)[25−30] to detect both polar and nonpolar molecules simultaneously and circumvent losses or alterations due to extraction. To the

DOI: 10.1021/acs.jproteome.7b00035
J. Proteome Res. 2017, 16, 1773−1783

best of our knowledge, this work is the first HRMAS NMR metabolomics report of the metabolic effects of Pd_2Spm on the human osteosarcoma MG-63 cell line as well as on osteoblasts (HOb cell line), the latter expressing the often overlooked response of healthy cells to the drug. Comparison to cDDP is carried out, and Pd_2Spm is evaluated in both single-drug protocols (in MG-63 and HOb cell lines) and combination protocols with doxorubicin (Dox) and methotrexate (Mtx) (in MG-63 cells), mimicking the presently used clinical chemotherapy cocktails and enabling drug synergisms to be identified.

EXPERIMENTAL SECTION

Chemicals and Solutions

Cisplatin was obtained from Sigma-Aldrich and doxorubicin and methotrexate from Fisher Scientific. Pd_2Spm was synthesized as previously reported.[31,32] For both single-drug and combination assays, initial stock solutions of cDDP (6.6 mM) and Pd_2Spm (1.5 mM) were prepared in phosphate-buffered saline (PBS) and PBS/DMSO (dimethyl sulfoxide) (10%), respectively. For drug combination assays, stock solutions of Dox (3.5 mM) and Mtx (8.8 mM) were prepared using Milli-Q H_2O and DMSO, respectively. All solutions were filtered (0.22 μm filter) and stored at 4 °C. Sulforhodamine B (SRB), PBS (pH 7.4), Hank's balanced salt solution (HBSS), DMSO, trypsin solution, Eagle's minimum essential medium (MEM), osteoblast basal medium, and osteoblast growth supplement were obtained from Sigma-Aldrich. Fetal bovine serum (FBS) was purchased from Gibco and the fluorescein isothiocyanate (FITC)-Annexin V apoptosis detection kit from BD Pharmingen.

Cell Culture and Drug Administration

The human MG-63 osteosarcoma cell line was kindly provided by the Associate Laboratory IBMC-INEB, Portugal. Cells were grown in monolayer in MEM culture medium, supplemented with 10% heat-inactivated FBS, 1 mM sodium pyruvate, 1 mM nonessential amino acids, and antibiotics (penicillin−streptomycin) and maintained under a humidified atmosphere at 5% CO_2 and 37 °C. Human osteoblasts (Sigma-Aldrich, HOb 406-06a cells) were grown in monolayer in Osteoblast Basal Medium supplemented with Osteoblast Growth Supplement and maintained under a humidified atmosphere at 5% CO_2 and 37 °C.

For single-drug exposure experiments (Figure 1b), MG-63 cells were seeded at a density of ~8×10^4 cells/cm^2 to provide sufficiently high cell density for NMR analysis. After waiting 24 h for cells to adhere, the experiment was initiated (t = 0 h) by adding stock solutions of each drug to achieve the respective IC_{50} concentrations (30 and 12 μM for cDDP and Pd_2Spm, respectively, as determined by the MTT assay for cDDP[33] and SRB for Pd_2Spm, as described in the following section). MG-63 cells were harvested at 12, 24, 36, and 48 h by trypsinization, washed with PBS, centrifuged (6 min, 1000 rpm, 21 °C), counted by the Trypan Blue assay, and stored at −80 °C until NMR analysis. HOb cells were seeded at a density of ca. 1.5×10^4 cells/cm^2 and, after 24 h, experiments were initiated (t = 0 h) by adding cDDP or Pd_2Spm stock solutions to achieve 30 and 12 μM, respectively; this will test, on healthy cells, the effects of the drugs' IC_{50} concentrations found for tumoral cells. At 0 and 24 h, cells were harvested by trypsinization, washed with HBSS, counted, centrifuged (5 min, 1200 rpm, 21 °C), and stored at −80 °C until NMR analysis. For the reversibility assays, the culture media in control and treated cells was removed after 24 h of drug exposure, and, after washing, the same volume of fresh, drug-free medium was added. After 3 days, cells were collected and stored for NMR analysis (Figure 1b). Two independent assays with duplicates for each condition (time point, drug, and recovery period) were performed for cell passages between 21 and 30 for MG-63 cells or 4 and 10 for HOb cells.

Drug combination assays were performed only for MG-63 cells (Figure 1c). Drug proportions and administration time scale were chosen to mimic as close as possible those used in the clinical European and American Osteosarcoma Studies (EURAMOS) protocol[34] while enabling a sufficiently high number of living cells to be obtained for NMR analysis. The IC_{50} concentration of Dox (3 μM at 24 h)[25] was used as reference to determine cDDP and Pd_2Spm dosages (4.8 μM) and Mtx (480 μM, in a first instance). Regarding the latter, additional adaptations were found to be necessary: (i) Only one Mtx addition was performed (instead of two as in the original EURAMOS protocol, thus enabling suitable cell numbers to be obtained for NMR analysis) and (ii) a Mtx 4.8 μM dosage was used instead of 480 μM because SRB assays of cDDP/Dox/Mtx cocktails with 4.8, 48, and 480 μM of Mtx revealed similar effects on cell proliferation (10.3, 12.3, and 10.3%, respectively, at 24 h of exposure to Mtx). After cells seeding and adhesion, experiments were initiated by adding cDDP (4.8 μM)/Dox (3 μM) or Pd_2Spm (4.8 μM)/Dox (3 μM) (Figure 1c), and cells were collected at 24, 48, and 72 h and handled as previously described. At 72 h, Mtx (4.8 μM) was added to cultures exposed to either cDDP/Dox or Pd_2Spm/Dox, and samples were collected after 24 h so that changes attributed to Mtx action alone could be assessed. At each time point, cells were harvested, washed, counted, centrifuged, and stored. Three independent assays, with duplicates for each condition (time point and drug cocktail), were performed for cell passages between 21 and 30.

Cytotoxicity and Apoptosis Assays

IC_{50} measurements for Pd_2Spm were performed by the SRB assay.[35−37] MG-63 cells were seeded on 24-well plates at 1×10^5 cell per well. After adhering (24 h), cells were treated with increasing doses of Pd_2Spm (1, 3, 5, 10, 15, 20, and 30 μM) and incubated for 12, 24, 36, 48, and 72 h, after which cells were washed twice with PBS and once with milli-Q H_2O (to remove the salt). The cells were fixed overnight with 2 mL/well of 1% acetic acid in methanol (2 mL/well) at −20 °C. Solvent excess was removed, and 1 mL of SRB 0.5% in acetic acid (w/v) was added to each well, followed by 1 h of incubation in the dark. Upon washing (1% acetic acid) and drying overnight at room temperature, the SRB bound to cellular proteins was dissolved (in a 10 mM Tris solution at pH 10) and quantified through the absorbance at 540 nm. Three independent experiments, with three replicates each, were performed. Cell densities (%) were determined according to cell density (%) = $(Abs_{treated} - Abs_{0h})/(Abs_{control} - Abs_{0h}) \times 100$. A Pd_2Spm concentration of 12.03 μM was found to inhibit 50% of MG-63 cell growth at 24 h (IC_{50} value at 24 h).

FITC-Annexin V, used in combination with propidium iodide (PI, vital dye with affinity for nucleic acids), enabled the simultaneous identification of different stages of apoptosis by flow cytometry. In brief, MG-63 cells were exposed to the IC_{50} concentrations of either cDDP or Pd_2Spm, and, after washing with PBS, cells were detached by trypsinization, cell suspensions were centrifuged twice (5 min, 2250 rpm, 4 °C),

DOI: 10.1021/acs.jproteome.7b00035
J. Proteome Res. 2017, 16, 1773−1783

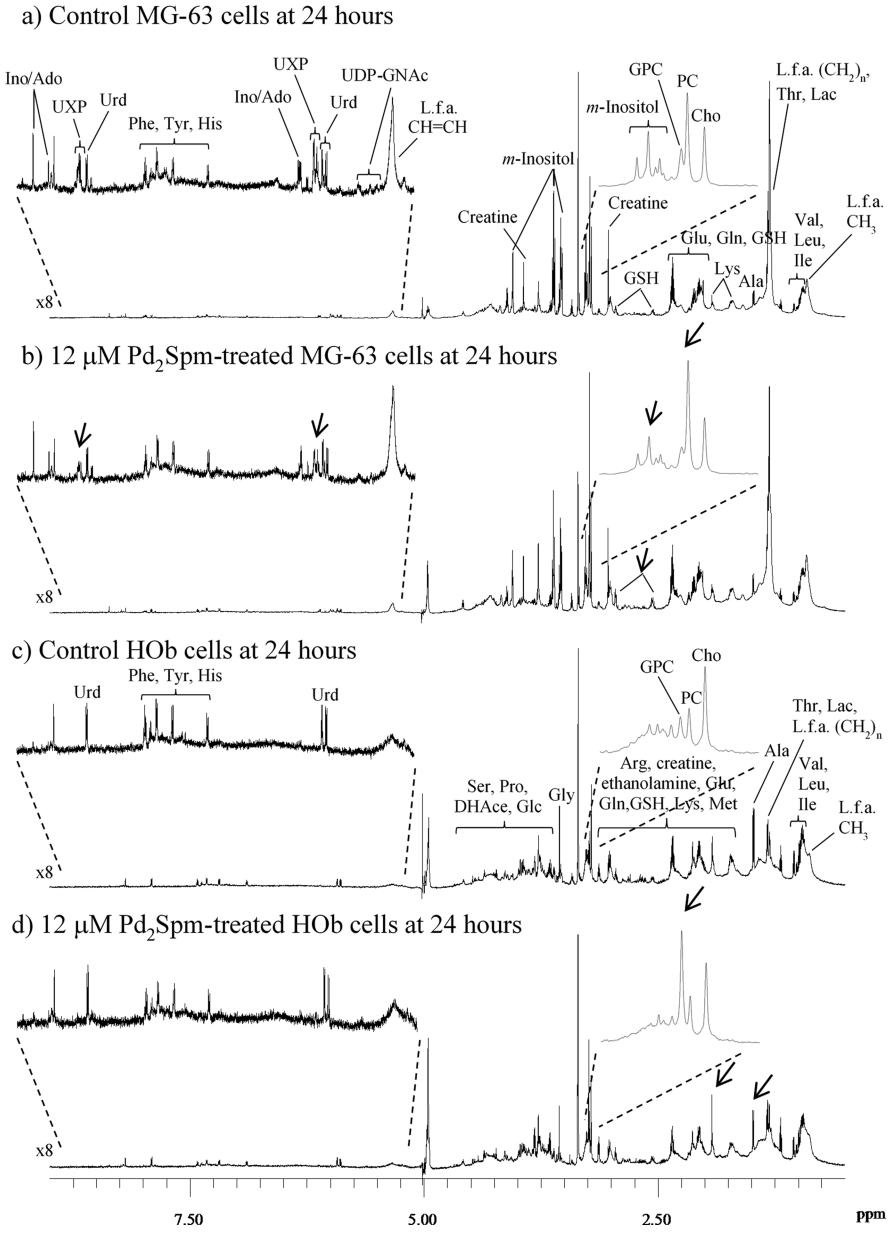

Figure 2. Average 800 MHz ^{1}H HRMAS NMR spectra of MG-63 cells (a,b) and HOb cells (c,d) at 24 h: (a,c) under control conditions and (b,d) exposed to 12 μM Pd_2Spm. Insets show expansions of choline compounds (3.2 to 3.3 ppm) and aromatic (5.15 to 8.5 ppm) regions. Main assignments are noted: three-letter code used for amino acids; Ado, adenosine; Cho, choline; DHAce, dihydroxyacetone; Glc, glucose; GPC, glycerophosphocholine; GSH, reduced glutathione; Ino, inosine; Lac, lactate; L.f.a., lipid fatty acyl groups; PC, phosphocholine; UDP-GNAc, uridine diphosphate acetylhexosamine; Urd, uridine; UXP, either of UDP/UTP/UDP-GNAc species. Arrows in panels b and d indicate visual spectral changes due to exposure to Pd_2Spm.

and 1 mL of PBS was added to the pellet. The protocol of the apoptosis detection kit supplier was applied. Finally, samples were subjected to flow cytometry for 1 h: at least 10000 events per sample were analyzed and the percentage of cells in each quadrant was estimated according to $cells_{quadrant}$ (%) = ($cells_{quadrant}/cells_{total}$) × 100.

NMR Spectroscopy

Samples were thawed and centrifuged, and cell pellets were suspended in 1 mL of PBS/D_2O (0.4 M NaCl, 0.0027 M KCl, 0.0015 M KH_2PO_4, 0.0081 M Na_2HPO_4 in D_2O, pH 7.4), centrifuged, and resuspended in 35 μL of PBS/D_2O, to which 5 μL of PBS/D_2O containing TSP-d_4 0.25% v/v was added. Then, a three-fold cycle of liquid nitrogen dipping and sonication was performed to lyse the cells,[38] and each sample was transferred to a sealed NMR disposable insert to be used in 4 mm MAS rotors (ca. 35 μL) and stored at −80 °C until analysis. Whenever needed, duplicates of the same condition were mixed together to achieve (5 to 10) × 10^6 cells and 1 × 10^6 cells for MG-63 and HOb (larger cells), respectively, to obtain suitable NMR signal-to-noise. The loaded inserts were placed in standard 4 mm MAS rotors and spectra were acquired on Bruker Avance spectrometers operating at either 800 MHz (single-drug assays) or 500 MHz (drug combination assays) for ^{1}H observation, at 277 K and 4 kHz spinning rate, using 4 mm HRMAS probes. 1D NMR spectra ("noesypr1d", Bruker library) were acquired for each sample with spectral width of 9803.92 Hz (single-drug and reversibility assays) or 6510.42 Hz

DOI: 10.1021/acs.jproteome.7b00035
J. Proteome Res. 2017, 16, 1773−1783

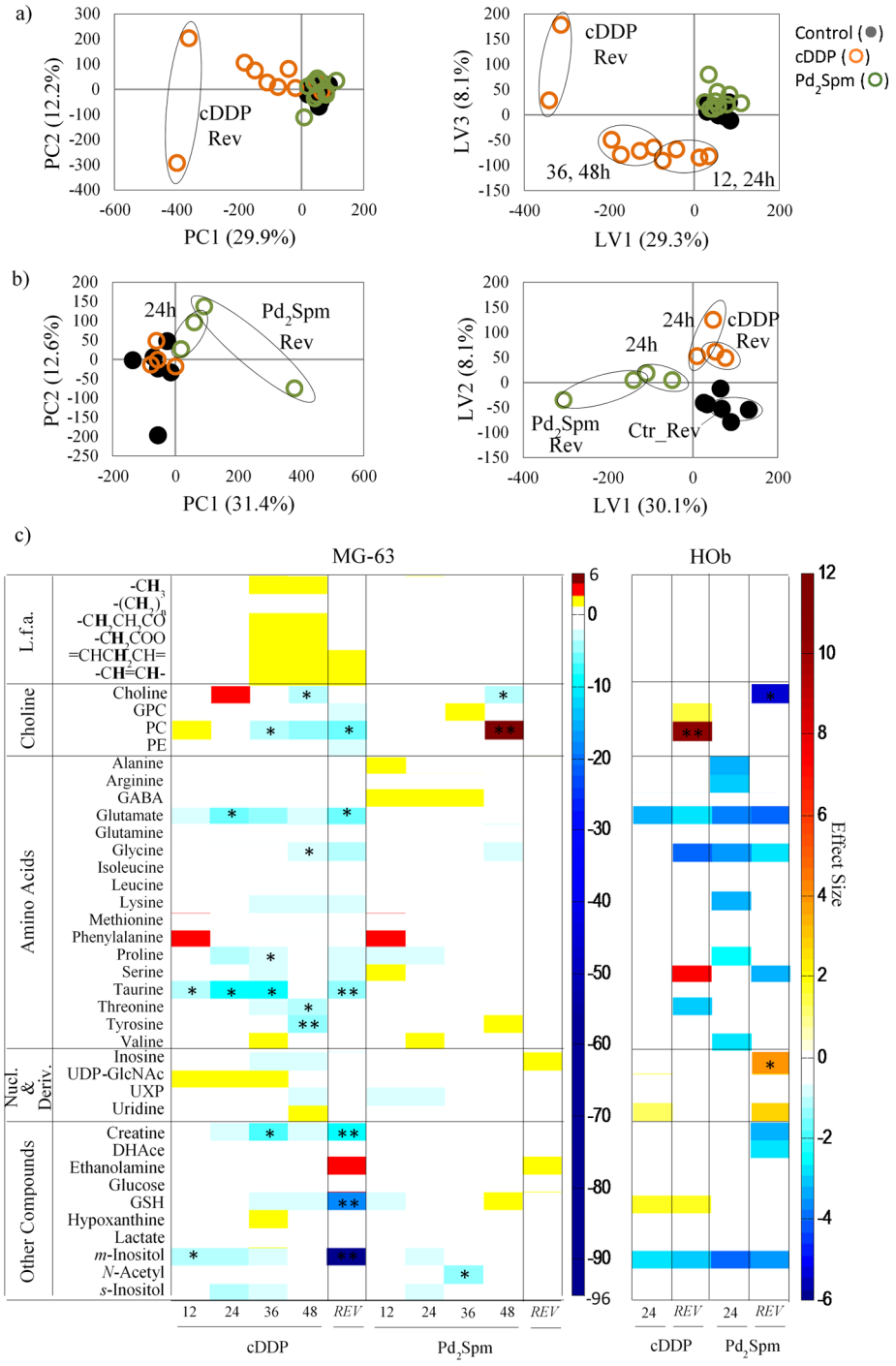

Figure 3. PCA (left) and PLS-DA (right) scores plots for (a) MG-63 cells and (b) HOb cells assays: controls (black full circles), cells treated with cDDP (open orange circles), or with Pd_2Spm (open green circles). (c) Color-coded heatmap representing the main metabolite changes (measured in effect size) observed for single-drug exposure assays on MG-63 and HOb cells. Columns marked *REV* correspond to results of reversibility assays. PE: phosphoethanolamine; UDP-GlcNAc, uridine diphosphate acetylglucosamine, *N*-acetyl, glycoprotein *N*-acetyl groups; other compound abbreviations as in Figure 2.

(drug combination assays) and 32 k data points. Relaxation delays and number of scans were 4 s and 256 for MG-63 cells and 2 s and 512 for HOb cells. All 1D spectra were processed with 0.3 Hz line broadening and 64 k zero filling, manually phased, and baseline-corrected. Chemical shifts were referenced internally to alanine at δ 1.48. Spectral assignment was based on 2D total correlation spectroscopy (TOCSY) and heteronuclear single quantum coherence (HSQC) spectra and consultation of spectral databases (Bruker Biorefcode database and the human metabolome database, HMDB)[39] and further supported by STOCSY[40] (MATLAB version 7.12.0, The MathWorks).

Data Processing and Analysis

In single-drug experiments, a total of 46 spectra were acquired, comprising 32 for MG-63 cells and 14 for HOb cells. For drug combination assays, 42 spectra were acquired, only for MG-63 cells. Data matrices were built from the 1D NMR spectra, excluding the water region (4.8 to 5.2 ppm). Spectral

DOI: 10.1021/acs.jproteome.7b00035
J. Proteome Res. 2017, 16, 1773−1783

processing and analysis were performed separately for each cell line, and the three different data matrices (single-drug/MG-63 cells, single-drug/HOb cells, and drug cocktail/MG-63 cells) were analyzed independently. The spectra were aligned using recursive segment wise peak alignment[41] and normalized by probabilistic quotient normalization (PQN)[42] (MATLAB 7.12.0, The MathWorks, Natick, MA). After unit variance scaling, principal component analysis (PCA) and partial least-squares discriminant analysis (PLS-DA) were applied (SIMCA-P 11.5, Umetrics, Sweden), employing Monte Carlo Cross Validation (MCCV) through a default seven-fold internal cross validation, from which Q^2 (predictive ability) and R^2 (explained variance) values were obtained. Selected NMR signals were integrated (Amix-Viewer software, Bruker, version 3.9.11), and effect size was calculated and adjusted for small sample numbers.[43] Statistical significances of metabolite variations were assessed by the two-sample t test (p value <0.05 considered for statistically significance). STOCSY[40] was performed (Matlab 7.12.0) for assignment and search of metabolic correlations.

RESULTS AND DISCUSSION

Single-Drug Assays: Metabolic Response of MG-63/HOb Cells to Pd_2Spm/cDDP

Cytotoxic evaluation conducted in parallel with NMR metabolomics through the Trypan Blue assay confirmed that 24 h exposure of MG-63 cells exposed to Pd_2Spm at 12 μM leads to ca. 50% of viability loss (Figure S1a, left, green bars), in agreement with SRB results. This reflects a viability decrease about twice as high as that observed for cDDP (IC_{50} 30 μM) and is in broad agreement with IC_{50} values reported for human tongue squamous cancer (19 μM)[23] and breast cancer (5−11 μM)[11] cell lines. However, for higher exposure periods and 3-day reversibility experiments, a partial recovery of neoplastic cells treated with Pd_2Spm is noted (probably due to cell repair processes), contrary to cDDP. On the contrary, osteoblasts' viability seems to be more affected by Pd_2Spm at 24 h than by cDDP, with apparent 3-day irreversibility for both drugs (Figure S1a, right).

The effect of 24 h of exposure to Pd_2Spm on the metabolic profile of MG-63 cells as viewed by NMR is weak (Figure 2a,b), compared with that observed for cDDP (Figure S2a,b). The latter is consistent with previous reports, namely, regarding significant increases in fatty acids (FAs) (de novo lipid biosynthesis and β-oxidation inhibition accompanying apoptosis), Cho, and glycerophosphocoline (GPC) (membrane degradation) and a decrease in *m*-inositol (osmoregulatory or antioxidative mechanisms).[25,29] Regarding Pd_2Spm, the spectra of 24-h-exposed MG-63 cells (Figure 2a,b) reveal a small decrease in the levels of *m*-inositol and UXP species and increases in phosphocholine (PC) and reduced glutathione (GSH), with no evidence of significantly enhanced lipid biosynthesis or membrane degradation (viewed through Cho and GPC). The different time-dependent impacts on MG-63 metabolism are clearly observed in PCA and PLS-DA score plots (Figure 3a), where Pd_2Spm-treated samples globally overlap with controls and cDDP-induced changes are clear and progressive, even after 3 days in drug-free medium (reversibility assays).

To compare the MG-63 cells behavior with that of healthy cells, the ^{1}H HRMAS spectrum of HOb cells (Figure 2c) was assigned for the first time to our knowledge (Table S1, over 40 identified metabolites). Compared with tumoral cells, HOb cells are poorer in lipids and exhibit a reversed PC/Cho ratio and a generally distinct profile of low M_w compounds (e.g., low levels or absence of inositol and UXP species). Exposure of HOb cells to Pd_2Spm induces a clear increase in GPC and minor changes across the spectrum (Figure 2c,d), whereas cDDP leaves the spectrum remarkably unchanged (Figure S2c,d). Indeed, time-course variations visualized in PCA and PLS-DA scores (Figure 3b) reflect some deviation of Pd_2Spm-treated HOb cells from controls, while cDDP-treated samples overlap largely with controls.

Pairwise PLS-DA scores and loadings analysis (not shown), followed by signal integration and effect size calculation (shown in Table S2 for 24 h, 48 h, and Mtx-addition), identified the metabolite variations underlying the multivariate analysis results. The lesser impact of Pd_2Spm on MG-63 metabolism, compared with cDDP, is clearer in the color-coded heat map (Figure 3c, only larger effect size variations) and time course graphs (Figure S3 (lipids and Cho compounds) and Figure S4 (other compounds)). Notably, lipid variations are absent, in both quantity and nature (average chain length, CH_2/CH_3, and unsaturation degree, $-HC{=}CH-/CH_3$, of fatty acyl chains). This suggests lack of apoptosis in Pd_2Spm-treated MG-63 cells, as subsequently confirmed by Annexin V assay results and contrary to cDDP-treated cells (Figure S1c,d). The very small changes in Cho and GPC (Figure S3) suggest the absence of membrane degradation and the small increase in PC and hence in PC/GPC ratio, in contrasts with the lower values of PC/GPC for cDDP (Figure S3), which have been related to cell growth arrest prior to apoptosis.[26] In addition, a few small amino acid changes are noted as a result of Pd_2Spm treatment (mainly in γ-aminobutyrate (GABA), phenylalanine, proline, tyrosine), together with lower levels of UXP and *m,s*-inositol and a small increase in GSH after 12 h (Figure 3c and Figure S4). These metabolic changes seem to be reversible for MG-63 cells treated with Pd_2Spm (Figure 3c), whereas cDDP induced continuing increases in lipids unsaturation, polyunsaturated FA species ($=CHCH_2CH=$) (without further lipids increase), and ethanolamine, along with decreases in six amino acids, GPC, PC, phosphoethanolamine (PE), creatine, GSH, and *m*-inositol. Interestingly, all nucleotide variations are, however, reverted in cDDP (Figure 3c), a possible indication that drug action on DNA has halted, leaving only longer term effects of drug exposure.

A similar approach for HOb cells, involving a single time collection at 24 h, identifies more metabolite changes with Pd_2Spm than with cDDP (Table S2, Figure 3c), with the former inducing marked amino acid decreases (possibly due to enhanced Krebs cycle activation or protein metabolism disturbances), small increases in lipids and GPC (although without relevant effect size variation, Table S2), and a noticeable absence of GSH change (suggestive of oxidative status maintenance in spite of drug action). The GPC increase leads to a lower PC/GPC ratio for Pd_2Spm at 24 h (0.46) compared with cDDP (0.88) and controls (0.89), thus suggesting enhanced HOb cell growth arrest upon Pd_2Spm treatment. Reversibility assays indicate lasting metabolic changes in HOb cells for both drugs, although cDDP-treated cells again recover nucleotide levels in drug-free medium (Figure 3c), contrary to Pd_2Spm-treated cells, where some indication of cell growth arrest remains (as shown by PC/GPC of 0.69, compared with 0.94 for controls).

DOI: 10.1021/acs.jproteome.7b00035
J. Proteome Res. 2017, 16, 1773−1783

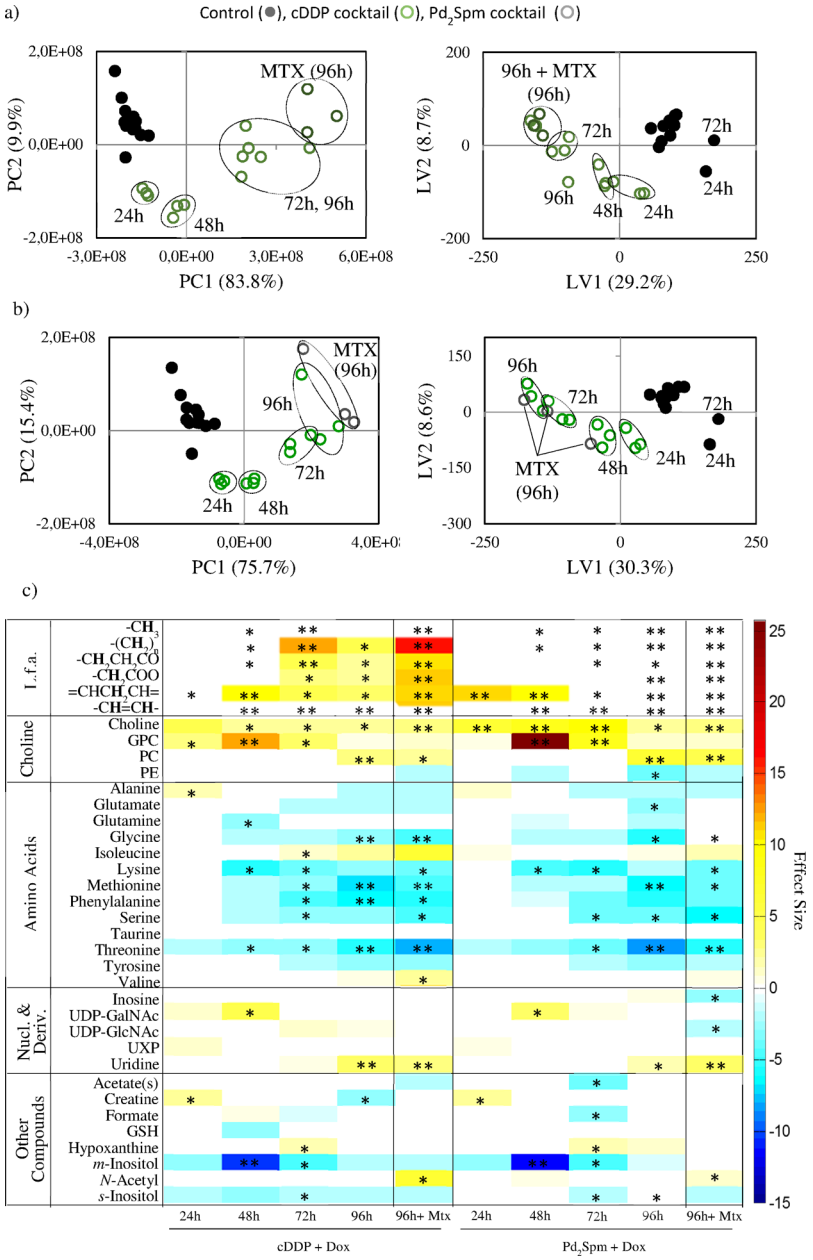

Figure 4. PCA (left) and PLS-DA (right) scores plots for MG-63 cells assays under control conditions (black full circles) and treated with (a) the cDDP/Dox/Mtx (open orange circles) and (b) the Pd_2Spm/Dox/Mtx cocktail (open green circles). (c) Color-coded heatmap representing the metabolite changes (measured in effect size) observed for drug combination assays on MG-63 cells. UDP-GalNAc, uridine diphosphate acetylgalactosamine; other compound abbreviations as in Figure 3.

The above results show that, although Pd_2Spm seems more cytotoxic to MG-63 cells than cDDP, at 24 h of exposure (lower IC_{50}), cells are not apoptotic and indeed seem to recover for longer times of exposure to the complex. Metabolically, Pd_2Spm contrasts with cDDP by only marginally altering MG-63 cell primary metabolism (impacting slightly PC/GPC, GABA, UXP species, GSH, and *m*-inositol), with the resulting small metabolite changes recovering well once the drug is removed. A contrasting metabolic behavior has, indeed, been registered by vibrational microspectroscopy,[32] with such study indicating that Pd_2Spm triggers unconventional cytotoxicity pathways in triple-negative human breast cancer compared with cDDP, probably due to different adducts formed with DNA (via long-range interstrand cross-links). However, the fact that the measurable impact of Pd_2Spm, viewed by NMR, is low compared with that measured by vibrational spectroscopy is not entirely clear in this stage, although the slower time scale of NMR measurements (10^{-1} to 10^{-9} s compared with 10^{-12} to 10^{-13} s for FTIR) and, hence, distinct observable molecular events may explain the above observations. On the contrary, we show that the Pd(II) complex induces more metabolic perturbations in osteoblasts (particularly in amino acids metabolism) compared with cDDP. This may constitute a drawback in terms of the use of Pd_2Spm, although the specific relationship between metabolic impact and effective drug cytotoxicity is not straightforward. In addition, both drugs seem to cause lasting metabolic changes in HOb cells (for 3 days after drug removal); however, this may also reflect the fact that drug intracellular concentrations in HOb cells are possibly

DOI: 10.1021/acs.jproteome.7b00035
J. Proteome Res. 2017, 16, 1773−1783

higher due to the lower cell density compared with MG-63 cells.

Drug Combination Assays: Metabolic Response of MG-63 Cells to Pd_2Spm/cDDP cocktails

The present study adds to recent reports of in vitro NMR metabolomics to measure and understand drug synergism in human colorectal cancer,[44] glioblastoma,[45] breast cancer,[46] and hepatocellular carcinoma.[47] The cytotoxicity results for MG-63 cells exposed to Pd_2Spm/Dox/Mtx and cDDP/Dox/Mtx cocktails (Figure S1b) reflect a remarkably similar behavior, with a steady decrease in number of viable cells at 96 h and prior to the late addition of Mtx. Mtx addition (at 72 h, followed by sample collection 24 h later) does not seem to impact cell viability, as viewed by the Trypan Blue assay. As for the impact of each cocktail on MG-63 metabolism, it is again clear that both cocktails display very similar behaviors, as assessed by PCA and PLS-DA of HRMAS spectra (Figure 4a,b), both defining a clear time trajectory away from control cells, with a clearer effect of the final addition of Mtx being noted for cDDP. Table S3 lists the corresponding metabolite changes, also represented in a heatmap (Figure 4c) and time-course graphs (Figures S5 and S6) for the sake of clarity. Results show that the Pd_2Spm cocktail induces marked increases and qualitative changes in lipids, increases in Cho, GPC (lowering PC/Cho and PC/GPC ratios), uridine, and derived species, and marked decreases in many amino acids and *m*-inositol. This expresses a strong synergetic effect, effectively enabling the Pd_2Spm complex to play a similar role in primary metabolism as cDDP when in cocktail form. Slight differences are noted in the reversibility column corresponding to the two cocktails (Figure 4c), namely regarding glutamate and threonine (closer to controls in Pd_2Spm), some nucleotide derivatives (remaining decreased in Pd_2Spm), and acetate and *m*-inositol (unchanged compared with controls, i.e., levels fully recovered).

Detailed comparison with the single-drug assays performed at each drug IC_{50} concentration for cDDP (30 μM, this work), Dox (3 μM),[25] and Mtx (3 μM)[25] enables other synergetic effects to be identified (noted in Table S3 for 24 h, 48 h, and Mtx addition) and summarized in Table 1). Because of the different drug concentrations used in the cocktails (for the metal agents and Mtx), compared with the single-drug assays, this identification can only be made qualitatively. Table 1 lists the main effects, at 48 h and upon Mtx addition, not expected in view of single-drug assays or simple addition of their effects. The strong Pd_2Spm/Dox synergism triggering lipids biosynthesis is further enhanced by Mtx, which induces a slight increase in lipid levels in both cocktails, leaving, however, polyunsaturated fatty acid (PUFA) levels (=$CHCH_2CH$=) unchanged. This effect of Mtx may be linked to the concomitant decrease in acetate (and perhaps to the small increases in the branched chain amino acids isoleucine and valine, Figure 4c), suggesting that Mtx may be synergistically triggering acetate-mediated FA synthesis. Other synergetic effects include changes in PC and PE (cDDP cocktail) and decreases in methionine and serine (both cocktails) and glutamine and valine (cDDP cocktail). Interestingly, both cocktails induce the production of UDP-GalNAc (uridine diphosphate acetylgalactosamine), which, together with UDP-GlcNAc (uridine diphosphate acetylgalactosamine) (enhanced by cDDP alone, but not by Pd_2Spm, Figure S4), is a substrate of lipids and proteins glycosylation.[48] Notably, a slight decrease

Table 1. Main Qualitative Synergetic Effects Observed (at 48 h and upon Mtx addition) in MG-63 Cells Exposed to cDDP(4.8 μM)/Dox(3 μM)/Mtx(4.8 μM) and Pd_2Spm(4.8 μM)/Dox(3 μM)/Mtx(4.8 μM) Cocktails by Comparison with Sole Administrations of cDDP (30 μM, this work), Dox (3 μM),[25] Mtx (3 μM),[25] and Pd_2Spm (12 μM, this work)[a]

MG-63 cells exposed to cDDP cocktail			
metabolite	δ (ppm)[b]	48 h (cDDP + Dox)	96 h (cDDP + Dox) + Mtx
Lipids			
$-C\underline{H}_3$	0.91		(+)
$-(C\underline{H}_2)_n$	1.30		(+)
$-C\underline{H}_2CH_2CO$	1.60		(+)
$-C\underline{H}_2COO$	2.25		(+)
$-C\underline{H}$=$C\underline{H}-$	5.33		(+)
Choline and Phospholipids			
PC	3.23, s		(+)
PE	3.25, s		(−)
Amino Acids			
glutamine	2.45, m	(−)	
methionine	2.13, s	(−)	
serine	3.84, d	(−)	
valine	1.05, d	(−)	
Nucleotides and Derivatives			
UDP-GalNAc	5.62, m	(+)	
Other Compounds			
acetate	1.92, s		(−)
formate	8.46, s	(+)	
N-acetyl	2.02, s		(+)
MG-63 Cells Exposed to Pd_2Spm Cocktail			
metabolite	δ (ppm)[b]	48 h (Pd_2Spm + Dox)	96 h (Pd_2Spm + Dox)+ Mtx
Lipids			
$-C\underline{H}_3$	0.91	(+)	
$-(C\underline{H}_2)_n$	1.30	(+)	
$-C\underline{H}_2CH_2CO$	1.60	(+)	(+)
$-C\underline{H}_2COO$	2.25	(+)	(+)
$-C\underline{H}$=$C\underline{H}-$	5.33	(+)	(+)
Amino Acids			
methionine	2.13, s	(−)	
serine	3.84, d	(−)	
Nucleotides and Derivatives			
inosine	8.36, s		(−)
UDP-GalNAc	5.62, m	(+)	
UDP-GlcNAc	5.52, m		(−)
Other Compounds			
hypoxanthine	8.18, s	(+)	

[a]Only effects not expected in view of single-drug assays or their additive effects are noted. [b]Resonance chosen for signal integration.

in UDP-GlcNAc in the cDDP cocktail suggests distinct roles for the two UDP-GNAc substrates. A direct mechanistic correlation of UDP-GNAc metabolites to lipids synthesis has been suggested in brain[27] and lung[30] tumor cells treated with cDDP but not confirmed in MG-63 cells.[25] Statistical total correlation spectroscopy (STOCSY) of the spectra obtained for cDDP/Dox (24, 48, 72, and 96 h) indicates no significant correlations of UDP-GalNAc to lipids (results not shown); however, upon the inclusion of the spectra obtained for cDDP/Dox/Mtx, a direct correlation between UDP-GalNAc and fatty acids becomes observable as well as an inverse correlation with

DOI: 10.1021/acs.jproteome.7b00035
J. Proteome Res. 2017, 16, 1773−1783

acetate, thus suggesting a specific role of Mtx in lipids biosynthetic pathways involving UDP-GalNAc. A similar result is obtained for the palladium cocktail, again reflecting a remarkably similar behavior of the Pd_2Spm complex to cDDP when in combination with Dox and Mtx.

CONCLUSIONS

Our results have shown that the Pd_2Spm complex presents an apparently higher cytotoxicity in MG-63 cells compared with cDDP. However, Pd_2Spm-treated osteosarcoma cells revealed a reversible, much lower metabolic impact on cellular metabolism (marked by the total absence of lipid biosynthesis and membrane degradation indicators) and, indeed, absence of apoptotic behavior. The apparent contradiction with the cytotoxicity results and lower IC_{50} of Pd_2Spm (12 μM compared with 30 μM for cDDP) raises an interesting question as to what cellular state is induced in Pd_2Spm-treated MG-63 cells, a subject for further investigation. Conversely, the Pd(II) agent importantly impacts osteoblast amino acid metabolism, resulting in persisting metabolic changes (at least for 3 days in drug-free media) similarly to cDDP. Subsequent combination of cDDP and Pd_2Spm with Dox and Mtx illustrated the well-recognized importance of using drug combinations rather than single-drug administration. Indeed, the combination of Pd_2Spm with Dox and Mtx triggered all of the deviant metabolic characteristics of cDDP action, producing an almost identical metabolic profile as that for the cDDP cocktail. The contrast in the metabolic effects of sole- and combined-administrations of Pd_2Spm suggests that the anticancer potential of this complex in osteosarcoma is more likely to arise when drug combination protocols are employed. Clear synergetic effects of the Pd_2Spm cocktail comprised changes in lipid biosynthesis, protein or lipid glycosylation involving UDP-GNAc substrates (and specifically UDP-GalNAc), and methionine and serine metabolisms. These pathways should therefore be the object of future more detailed targeted studies. Finally, testing of the combination of these drugs on osteoblasts should also follow, necessarily circumventing their characteristic slow cell growth rates and subsequent difficulty in obtaining large enough cell numbers for metabolomic analysis.

ASSOCIATED CONTENT

Supporting Information

The Supporting Information is available free of charge on the ACS Publications website at DOI: 10.1021/acs.jproteome.7b00035.

Figure S1. Cytotoxicity results for single drug and drug combination assays and results of flow cytometry assays of control and cisplatin/Pd_2Spm-treated cells. Figure S2. Average 800 MHz ^{1}H HRMAS NMR spectra of MG-63 cells and HOb cells at 24 h. Figure S3. Time course graphs of lipids and choline compounds, obtained for MG-63 cells in control conditions and treated with 30 μM cDDP or with 12 μM Pd_2Spm. Figure S4. Time course graphs of amino acids, nucleotides and derivatives, and other compounds/peaks obtained for MG-63 cells in control conditions and treated with 30 μM cDDP or with 12 μM Pd_2Spm. Figure S5. Time course graphs of lipids and choline compounds obtained for MG-63 cells in control conditions and treated with the cDDP/Dox/Mtx or Pd_2Spm/Dox/Mtx cocktails. Figure S6. Time course graphs of amino acids, nucleotides and derivatives, and other compounds/peaks obtained for MG-63 cells in control conditions and treated with the cDDP/Dox/Mtx or Pd_2Spm/Dox/Mtx cocktails. Table S1. Peak assignments on the ^{1}H HRMAS spectrum of HOb cells. Table S2. Metabolite variations in MG-63 cells and HOb cells exposed to 30 μM cDDP or 12 μM Pd_2Spm for 24 and 48 h and after the 3 day reversibility period compared with control cells. Table S3. Metabolite variations in MG-63 cells exposed to the cDDP/Dox/Mtx cocktail for 24, 48, 72, and 96 h compared to control cells. (PDF)

AUTHOR INFORMATION

Corresponding Author

*Phone: +351 234 370707. Fax +351 234 370084. E-mail: agil@ua.pt.

ORCID

Ana M. Gil: 0000-0003-3766-4364

Notes

The authors declare no competing financial interest.

ACKNOWLEDGMENTS

This work was developed within the scope of the project CICECO-Aveiro Institute of Materials (ref. FCT/UID/CTM/50011/2013), financed by national funds through the FCT/MEC and cofinanced by FEDER under the PT2020 Partnership Agreement. We acknowledge financial support from the Portuguese Foundation for Science and Technology: PTDC/QEQ-MED/1890/2014, within Project 3599, to Promote Scientific Production and Technological Development, as well as the formation of thematic networks (3599-PPCDT), jointly financed by the European Community Fund FEDER. FCT funds are also acknowledged from UID/MULTI/00070/2013 (R&D Group "Molecular Physical-Chemistry", University of Coimbra), PTDC/SAL-BEB/66896/2006, SFRH/BD/63916/2009, SFRH/BD/111576/2015, and SFRH/BPD/111736/2015 grants and from the Portuguese National NMR Network (RNRMN). We thank the Associate Laboratory IBMC-INEB for kindly providing the MG-63 cell line, and I.F.D. acknowledges FCT/MCTES for a research contract under the "Investigador FCT" 2014 Program.

REFERENCES

(1) Rosenberg, B.; VanCamp, L.; Trosko, J. E.; Mansour, V. H. Platinum compounds: a new class of potent antitumour agents. *Nature* **1969**, *222* (5191), 385−386.

(2) Wiltshaw, E. Cisplatin in the treatment of cancer. *Platinum Met. Rev.* **1979**, *23* (3), 90−98.

(3) Wheate, N. J.; Walker, S.; Craig, G. E.; Oun, R. The status of platinum anticancer drugs in the clinic and in clinical trials. *Dalton Trans.* **2010**, *39* (35), 8113−8127.

(4) Lovejoy, K. S.; Lippard, S. J. Non-traditional platinum compounds for improved accumulation, oral bioavailability, and tumor targeting. *Dalton Trans.* **2009**, *48*, 10651−10659.

(5) Kostova, I. Ruthenium complexes as anticancer agents. *Curr. Med. Chem.* **2006**, *13* (9), 1085−1107.

(6) Braga, S. S.; Marques, J.; Heister, E.; Diogo, C. V.; Oliveira, P. J.; Paz, F. A. A.; Santos, T. M.; Marques, M. P. M. Carriers for metal complexes on tumour cells: the effect of cyclodextrins vs CNTs on the model guest phenanthroline-5,6-dione trithiacyclononane ruthenium-(II) chloride. *BioMetals* **2014**, *27* (3), 507−525.

(7) Kostova, I. Titanium and vanadium complexes as anticancer agents. *Anti-Cancer Agents Med. Chem.* **2009**, *9* (8), 827−842.

DOI: 10.1021/acs.jproteome.7b00035
J. Proteome Res. 2017, 16, 1773−1783

(8) Messori, L.; Scaletti, F.; Massai, L.; Cinellu, M. A.; Gabbiani, C.; Vergara, A.; Merlino, A. The mode of action of anticancer gold-based drugs: a structural perspective. *Chem. Commun. (Cambridge, U. K.)* **2013**, *49* (86), 10100−10102.
(9) Ray, S.; Mohan, R.; Singh, J. K.; Samantaray, M. K.; Shaikh, M. M.; Panda, D.; Ghosh, P. Anticancer and antimicrobial metallopharmaceutical agents based on palladium, gold, and silver N-heterocyclic carbene complexes. *J. Am. Chem. Soc.* **2007**, *129* (48), 15042−15053.
(10) Marques, M. P. M. Platinum and palladium polyamine complexes as anticancer agents: the structural factor. *ISRN Spectrosc.* **2013**, *2013*, 1−29.
(11) Fiuza, S. M.; Holy, J.; Batista de Carvalho, L. A. E.; Marques, M. P. M. Biologic activity of a dinuclear Pd(II)-spermine complex toward human breast cancer. *Chem. Biol. Drug Des.* **2011**, *77* (6), 477−488.
(12) Silva, T. M.; Andersson, S.; Sukumaran, S. K.; Marques, M. P.; Persson, L.; Oredsson, S. Norspermidine and Novel Pd(II) and Pt(II) Polynuclear Complexes of Norspermidine as Potential Antineoplastic Agents Against Breast Cancer. *PLoS One* **2013**, *8* (2), e55651.
(13) Silva, T. M.; Fiuza, S. M.; Marques, M. P. M.; Persson, L.; Oredsson, S. Increased breast cancer cell toxicity by palladination of the polyamine analogue N (1),N (11)-bis(ethyl)norspermine. *Amino Acids* **2014**, *46* (2), 339−352.
(14) Giovagnini, L.; Ronconi, L.; Aldinucci, D.; Lorenzon, D.; Sitran, S.; Fregona, D. Synthesis, characterization, and comparative in vitro cytotoxicity studies of platinum(II), palladium(II), and gold(III) methylsarcosinedithiocarbamate complexes. *J. Med. Chem.* **2005**, *48* (5), 1588−1595.
(15) Kapdi, A. R.; Fairlamb, I. J. S. Anti-cancer palladium complexes: a focus on PdX2L2, palladacycles and related complexes. *Chem. Soc. Rev.* **2014**, *43* (13), 4751−4777.
(16) Komeda, S. Unique platinum-DNA interactions may lead to more effective platinum-based antitumor drugs. *Metallomics* **2011**, *3* (7), 650−655.
(17) Malina, J.; Farrell, N. P.; Brabec, V. DNA condensing effects and sequence selectivity of DNA binding of antitumor noncovalent polynuclear platinum complexes. *Inorg. Chem.* **2014**, *53* (3), 1662−1671.
(18) Qu, Y.; Kipping, R. G.; Farrell, N. P. Solution studies on DNA interactions of substitution-inert platinum complexes mediated via the phosphate clamp. *Dalton Trans.* **2015**, *44* (8), 3563−3572.
(19) Brabec, V.; Kasparkova, J. Modifications of DNA by platinum complexes. Relation to resistance of tumors to platinum antitumor drugs. *Drug Resist. Updates* **2005**, *8* (3), 131−146.
(20) Nowotarski, S. L.; Woster, P. M.; Casero, R. A. Polyamines and cancer: implications for chemotherapy and chemoprevention. *Expert Rev. Mol. Med.* **2013**, *15*, e3.
(21) Navarro-Ranninger, C.; Pérez, J.; Zamora, F.; González, V.; Masaguer, J.; Alonso, C. Palladium (II) compounds of putrescine and spermine. Synthesis, characterization, and DNA-binding and antitumor properties. *J. Inorg. Biochem.* **1993**, *52* (1), 37−49.
(22) Tummala, R.; Diegelman, P.; Fiuza, S. M.; Batista de Carvalho, L. A. E.; Marques, M. P. M.; Kramer, D. L.; Clark, K.; Vujcic, S.; Porter, C. W.; Pendyala, L. Characterization of Pt-, Pd-spermine complexes for their effect on polyamine pathway and cisplatin resistance in A2780 ovarian carcinoma cells. *Oncol. Rep.* **2010**, *24* (1), 15−24.
(23) Soares, A.; Fiuza, S.; Goncalves, M.; Batista de Carvalho, L.; Marques, M. P.; Urbano, A. Effect of the metal center on the antitumor activity of the analogous dinuclear spermine chelates (PdCl2)2(spermine) and (PtCl2)2(spermine). *Lett. Drug Des. Discovery* **2007**, *4* (7), 460−463.
(24) Corduneanu, O.; Chiorcea-Paquim, A.; Fiuza, S. M.; Marques, M.; Oliveira-Brett, A. Polynuclear palladium complexes with biogenic polyamines: AFM and voltammetric characterization. *Bioelectrochemistry* **2010**, *78* (2), 97−105.
(25) Lamego, I.; Duarte, I. F.; Marques, M. P. M.; Gil, A. M. Metabolic markers of MG-63 osteosarcoma cell line response to doxorubicin and methotrexate treatment: comparison to cisplatin. *J. Proteome Res.* **2014**, *13* (12), 6033−6045.
(26) Mirbahai, L.; Wilson, M.; Shaw, C. S.; McConville, C.; Malcomson, R. D. G.; Griffin, J. L.; Kauppinen, R. A.; Peet, A. C. 1H magnetic resonance spectroscopy metabolites as biomarkers for cell cycle arrest and cell death in rat glioma cells. *Int. J. Biochem. Cell Biol.* **2011**, *43* (7), 990−1001.
(27) Pan, X.; Wilson, M.; Mirbahai, L.; McConville, C.; Arvanitis, T. N.; Griffin, J. L.; Kauppinen, R. A.; Peet, A. C. In vitro metabonomic study detects increases in UDP-GlcNAc and UDP-GalNAc, as early phase markers of cisplatin treatment response in brain tumor cells. *J. Proteome Res.* **2011**, *10* (8), 3493−3500.
(28) Vermathen, M.; Paul, L. E. H.; Diserens, G.; Vermathen, P.; Furrer, J. 1H HR-MAS NMR based metabolic profiling of cells in response to treatment with a hexacationic ruthenium metallaprism as potential anticancer drug. *PLoS One* **2015**, *10* (5), e0128478.
(29) Duarte, I. F.; Lamego, I.; Marques, J.; Marques, M. P. M.; Blaise, B. J.; Gil, A. M. Nuclear magnetic resonance (NMR) study of the effect of cisplatin on the metabolic profile of MG-63 osteosarcoma cells. *J. Proteome Res.* **2010**, *9* (11), 5877−5886.
(30) Duarte, I. F.; Ladeirinha, A. F.; Lamego, I.; Gil, A. M.; Carvalho, L.; Carreira, I. M.; Melo, J. B. Potential markers of cisplatin treatment response unveiled by NMR metabolomics of human lung cells. *Mol. Pharmaceutics* **2013**, *10* (11), 4242−4251.
(31) Codina, G.; Caubet, A.; López, C.; Moreno, V.; Molins, E. Palladium(II) and Platinum(II) Polyamine Complexes: X-Ray Crystal Structures of (SP-4−2)-Chloro{N-[(3-amino-κN)propyl]propane-1,3-diamine-κN,κN′}palladium(1+) Tetrachloropalladate (2-) (2:1) and (R,S)-Tetrachloro[μ-(spermine)]dipalladium(II) (={μ-{N,N′-. *Helv. Chim. Acta* **1999**, *82* (7), 1025−1037.
(32) Batista de Carvalho, A. L. M.; Pilling, M.; Gardner, P.; Doherty, J.; Cinque, G.; Wehbe, K.; Kelley, C.; Batista de Carvalho, L. A. E.; Marques, M. P. M. Chemotherapeutic response to cisplatin-like drugs in human breast cancer cells probed by vibrational microspectroscopy. *Faraday Discuss.* **2016**, *187* (0), 273−298.
(33) Mosmann, T. Rapid colorimetric assay for cellular growth and survival: Application to proliferation and cytotoxicity assays. *J. Immunol. Methods* **1983**, *65* (1−2), 55−63.
(34) Whelan, J. S.; Bielack, S. S.; Marina, N.; Smeland, S.; Jovic, G.; Hook, J. M.; Krailo, M.; Anninga, J.; Butterfass-Bahloul, T.; Böhling, T.; et al. EURAMOS-1, an international randomised study for osteosarcoma: Results from pre-randomisation treatment. *Ann. Oncol.* **2015**, *26* (2), 407−414.
(35) Skehan, P.; Storeng, R.; Scudiero, D.; Monks, A.; McMahon, J.; Vistica, D.; Warren, J. T.; Bokesch, H.; Kenney, S.; Boyd, M. R. New colorimetric cytotoxicity assay for anticancer-drug screening. *JNCI J. Natl. Cancer Inst.* **1990**, *82* (13), 1107−1112.
(36) Voigt, W. Sulforhodamine B assay and chemosensitivity. *Methods Mol. Med.* **2005**, *110*, 39−48.
(37) Vichai, V.; Kirtikara, K. Sulforhodamine B colorimetric assay for cytotoxicity screening. *Nat. Protoc.* **2006**, *1* (3), 1112−1116.
(38) Duarte, I. F.; Marques, J.; Ladeirinha, A. F.; Rocha, C.; Lamego, I.; Calheiros, R.; Silva, T. M.; Marques, M. P. M.; Melo, J. B.; Carreira, I. M.; Gil, A. M. Analytical approaches toward successful human cell metabolome studies by NMR spectroscopy. *Anal. Chem.* **2009**, *81* (12), 5023−5032.
(39) Wishart, D. S.; Tzur, D.; Knox, C.; Eisner, R.; Guo, A. C.; Young, N.; Cheng, D.; Jewell, K.; Arndt, D.; Sawhney, S.; et al. HMDB: the Human Metabolome Database. *Nucleic Acids Res.* **2007**, *35*, D521−D526.
(40) Cloarec, O.; Dumas, M.-E.; Craig, A.; Barton, R. H.; Trygg, J.; Hudson, J.; Blancher, C.; Gauguier, D.; Lindon, J. C.; Holmes, E.; et al. Statistical total correlation spectroscopy: an exploratory approach for latent biomarker identification from metabolic 1H NMR data sets. *Anal. Chem.* **2005**, *77* (5), 1282−1289.
(41) Veselkov, K. A.; Lindon, J. C.; Ebbels, T. M. D.; Crockford, D.; Volynkin, V. V.; Holmes, E.; Davies, D. B.; Nicholson, J. K. Recursive segment-wise peak alignment of biological (1)H NMR spectra for

DOI: 10.1021/acs.jproteome.7b00035
J. Proteome Res. 2017, 16, 1773−1783

improved metabolic biomarker recovery. *Anal. Chem.* **2009**, *81* (1), 56−66.
(42) Dieterle, F.; Ross, A.; Schlotterbeck, G.; Senn, H. Probabilistic quotient normalization as robust method to account for dilution of complex biological mixtures. Application in 1H NMR metabonomics. *Anal. Chem.* **2006**, *78* (13), 4281−4290.
(43) Berben, L.; Sereika, S.; Engberg, S. Effect size estimation: methods and examples. *Int. J. Nurs. Stud.* **2012**, *49* (8), 1039−1047.
(44) Bradshaw-Pierce, E. L.; Pitts, T. M.; Kulikowski, G.; Selby, H.; Merz, A. L.; Gustafson, D. L.; Serkova, N. J.; Eckhardt, S. G.; Weekes, C. D. Utilization of quantitative in vivo pharmacology approaches to assess combination effects of everolimus and irinotecan in mouse xenograft models of colorectal cancer. *PLoS One* **2013**, *8* (3), e58089.
(45) Cuperlovic-Culf, M.; Touaibia, M.; St-Coeur, P.-D.; Poitras, J.; Morin, P.; Culf, A. S. Metabolic effects of known and novel HDAC and SIRT inhibitors in glioblastomas independently or combined with Temozolomide. *Metabolites* **2014**, *4* (3), 807−830.
(46) Lefort, N.; Brown, A.; Lloyd, V.; Ouellette, R.; Touaibia, M.; Culf, A.; Cuperlovic-Culf, M. ^{1}H NMR metabolomics analysis of the effect of dichloroacetate and allopurinol on breast cancers. *J. Pharm. Biomed. Anal.* **2014**, *93*, 77−85.
(47) Zheng, J.-F.; Lu, J.; Wang, X.-Z.; Guo, W.-H.; Zhang, J.-X. Comparative metabolomic profiling of hepatocellular carcinoma cells treated with sorafenib monotherapy vs. sorafenib-everolimus combination therapy. *Med. Sci. Monit.* **2015**, *21*, 1781−1791.
(48) Butkinaree, C.; Park, K.; Hart, G. O-linked beta-N-acetylglucosamine (O-GlcNAc): Extensive crosstalk with phosphorylation to regulate signaling and transcription in response to nutrients and stress. *Biochim. Biophys. Acta, Gen. Subj.* **2010**, *1800* (2), 96−106.

DOI: 10.1021/acs.jproteome.7b00035
J. Proteome Res. 2017, 16, 1773−1783